Nanostructure and Transition of a Strong Polyelectrolyte Brush at the Air/Water Interface †

ARTICLE *in* LANGMUIR · FEBRUARY 2007

Impact Factor: 4.46 · DOI: 10.1021/la061444x · Source: PubMed

3 AUTHORS, INCLUDING:

Ploysai Ohama
Suan Sunandha Rajabhat University
13 PUBLICATIONS **240** CITATIONS
SEE PROFILE

Kozo Matsumoto
Kinki University
123 PUBLICATIONS **1,537** CITATIONS
SEE PROFILE

Nanostructure and Transition of a Strong Polyelectrolyte Brush at the Air/Water Interface†

Ploysai Kaewsaiha, Kozo Matsumoto, and Hideki Matsuoka*

Department of Polymer Chemistry, Kyoto University, Kyoto, 615-8510, Japan

The strong polyelectrolyte layer in the monolayer of ionic amphiphilic diblock copolymers at the air/water interface consists of carpet and brush layers when the brush density is satisfactorily high like that of the weak acid polymer. Also, a drastic structural change was induced by the addition of salt to the brush layer. In this study, the critical brush density for the transition between "carpet-only" and "carpet + brush" structures for the strongly ionic amphiphilic diblock copolymer, poly(hydrogenated isoprepene)-*b*-poly(styrene sulfonic acid) sodium salt, monolayer was measured by an in situ X-ray reflectivity technique. The critical brush density was found to be about 0.12 nm^{-2}, which is lower than that observed for a weak acid polymer and, unlike the weak acid polymer, is independent of the hydrophilic chain length. This difference might be attributed to the strong ionic nature of the brush chain. In addition, the reversibility of the transition was confirmed. The effect of salt addition to the nanostructure of the carpet layer was examined in detail. No structural change was found, indicating that most of the ionic groups in the carpet layer do not show an ionic nature because of counterion condensation.

1. Introduction

Polyelectrolytes are widely used in cosmetics, food, paints, and biomedical devices. Polyelectrolyte chains anchored on a surface (i.e., polyelectrolyte brushes[1−6]) also have attracted attention for their expected wide possibility of applications. They can modify surface properties, for example, lower the surface tension, preventing the adsorption of proteins on surface,[7] enhance the stability of colloidal particles,[8−12] reducing friction,[13] and may be used to prepare drug-release systems.[14]

Ionic amphiphilic diblock copolymers[15] have the characteristics of polymers, ions, and amphiphiles and can self-assemble to the surface when their hydrophobic chains are suitably long[16] to form a monolayer.[17] When they densely tether to the surface, the hydrophilic part can be regarded as a polyelectrolyte brush. The properties of such polyelectrolyte brushes have been investigated theoretically[18,19] and experimentally.[20−29] Our previous work and that of Helm et al.[28] showed that the ionic hydrophilic layer in a monolayer at the air/water interface is not a simple layer but consists of a high-density layer just beneath the water surface and a brushlike layer below it.[22−29] We consider that the high-density layer, which we call the "carpet layer", is formed to reduce the interfacial free energy between the hydrophobic layer and water. The carpet layer has an almost constant thickness of 10−20 Å, independent of the surface pressure and hydrophilic chain length. However, the brush layer thickness increased with increasing surface pressure, namely, with increasing polymer brush density. The hydrophobic layer thickness also increased by compression. The brush layer formed only when the brush density was satisfactorily high and the hydrophilic chain length was long enough.[25] In other cases, only a carpet layer was formed. We previously estimated the critical brush density for the transition from the "carpet-only" layer structure to the "carpet + brush" double-layer structure of a weakly ionic amphiphilic diblock copolymer.[27]

† Part of the Stimuli-Responsive Materials: Polymers, Colloids, and Multicomponent Systems special issue.

* To whom correspondence should be addressed. E-mail: matsuoka@star.polym.kyoto-u.ac.jp.

(1) De Gennes, P. G. *Macromolecules* **1980**, *13*, 1069.
(2) Milner, S. T. *Science* **1991**, *251*, 905.
(3) (a) Halperin, A.; Tirrell, M.; Lodge, T. P. *Adv. Polym. Sci.* **1992**, *100*, 31. (b) Advincula, R. C., Brittain, W. J., Claster, K. C., Rühe, J., Eds. Polymer Brushes; Wiley: New York, 2004.
(4) Zhao, B.; Brittain, W. J. *J. Am. Chem. Soc.* **1999**, *121*, 3557.
(5) Tran, Y.; Auroy, P.; Lee, L. T. *Macromolecules* **1999**, *32*, 8952.
(6) Lemieux, M.; Usov, D.; Minko, S.; Stamm, M.; Shulha, H.; Tsukruk, V. V. *Macromolecules* **2003**, *36*, 7244.
(7) Carignano, M. A.; Szleifer, I. *Colloids Surf., B* **2000**, *18*, 169.
(8) Wittemann, A.; Drechsler, M.; Talmon, Y.; Ballauff, M. *J. Am. Chem. Soc.* **2005**, *127*, 9688.
(9) Leemans, L.; Fayt, R.; Teyssié, Ph. *Macromolecules* **1991**, *24*, 5922.
(10) Mohanty, P. S.; Harada, T.; Matsumoto, K.; Matsuoka, H. *Macromolecules* **2006**, *39*, 2016.
(11) Matsuoka, H.; Maeda, S.; Kaewasaiha, P.; Matsumoto, K. *Langmuir* **2004**, *20*, 7412.
(12) Matsumoto, H.; Hasegawa, H.; Matsuoka, M. *Tetrahedron* **2004**, *60*, 7197.
(13) Raviv, U.; Glasson, S.; Kampf, N.; Gohy, J. F.; Jerome, R.; Klein, J. *Nature* **2003**, *425*, 163.
(14) Zhu, X.; DeGraaf, J.; Winnik, F. M.; Leckband, D. *Langmuir* **2004**, *20*, 10656.
(15) Hamley, I. W. *Block Copolymers in Solution: Fundamentals and Applications*; Wiley: New York, 2005; Chapter 5.
(16) Kaewsaiha, P.; Matsumoto, K.; Matsuoka, H. *Langmuir* **2005**, *21*, 9938.
(17) Kaewsaiha, P.; Matsumoto, K.; Matsuoka, H. *Langmuir* **2004**, *20*, 6754.
(18) Pincus, P. A. *Macromolecules* **1991**, *24*, 2912.
(19) (a) Israels, R.; Leermarkers, F. A. M.; Fleer, G. J.; Zhulina, E. B. *Macromolecules* **1994**, *27*, 3249. (b) Borisov, O. V.; Zhulina, E. B.; Birstein T. M. *Macromolecules* **1994**, *27*, 4795.
(20) Su, T. J.; Styrkas, D. A.; Thomas, R. K.; Baines, F. L.; Billingham, N. C.; Armes, S. P. *Macromolecules* **1996**, *29*, 6892.
(21) An, S. W.; Su, T. J.; Thomas, R. K.; Baines, F. L.; Billingham, N. C.; Armes, S. P.; Penfold, J. *J. Phys. Chem. B* **1998**, *102*, 387.
(22) Mouri, E.; Matsumoto, K.; Matsuoka, H. J. *Polym. Sci., Part B* **2003**, *41*, 1921.
(23) Mouri, E.; Matsumoto, K.; Matsuoka, H. *J. Appl. Crystallogr.* **2003**, *36*, 722.
(24) Mouri, E.; Kaewsaiha, P.; Matsumoto, K.; Matsuoka, H.; Torikai, N. *Langmuir* **2004**, *20*, 10604.
(25) Mouri, E.; Furuya, Y.; Matsumoto, K.; Matsuoka, H. *Langmuir* **2004**, *20*, 8062.
(26) Mouri, E.; Matsumoto, K.; Matsuoka, H.; Torikai, N. *Langmuir* **2005**, *21*, 1840.
(27) (a) Matsuoka, H.; Furuya, Y.; Kaewsaiha, P.; Matsumoto, K. *Langmuir* **2005**, *21*, 6845. (b) Matsuoka, H.; Furuya, Y.; Kaewsaiha, P.; Matsumoto, K. *Langmuir*, submitted for publication.
(28) (a) Ahrens, H.; Forster, H.; Helm, C. A. *Macromolecules* **1997**, *30*, 8447. (b) Ahrens, H.; Forster, H.; Helm, C. A. *Phys. Rev. Lett.* **1998**, *81*, 4172. (c) Ahrens, H.; Forster, H.; Helm, C.; Kumar, A. K.; Naji, A.; Netz, R. R.; Seidel, C. *J. Phys. Chem. B* **2004**, *108*, 16870.
(29) Yim, H.; Kent, M. S.; Huber, D.; Satija, S.; Majewski, J.; Smith, G. S. *Macromolecules* **2003**, *36*, 5244.

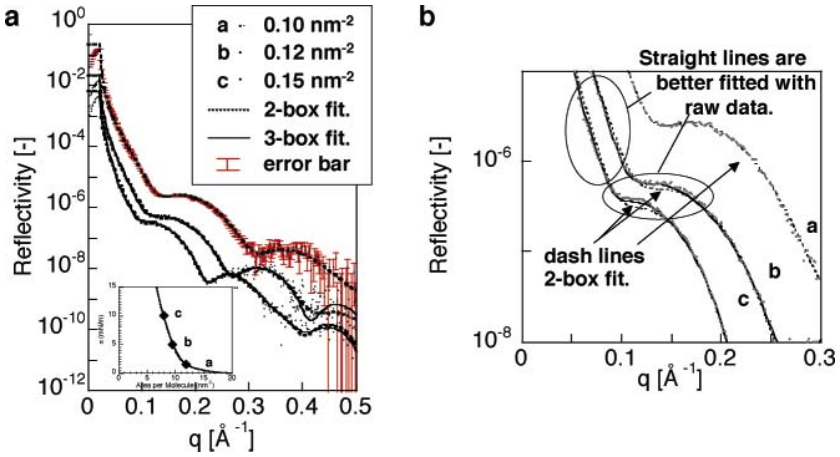

Figure 1. (a) X-ray reflectivity of (Ip-h$_2$)$_{220}$-*b*-(SS)$_{55}$ monolayers on water along the isotherm shown in the inset. Each curve was shifted downward for clarity. Dashed lines are for the two-box model, and the solid line is for the three-box model. (b) Magnification of part a in a small-*q* range showing the difference between two fitting models.

Table 1. Characteristics of (Ip-h$_2$)$_m$-*b*-(SS)$_n$ Block Copolymers

m/n	M_n	M_w/M_n	degree of sulfonation
180:17	15 300	1.03	0.68
215:31	20 600	1.10	0.92
220:55	25 000	1.11	0.87
209:115	33 000	1.24	0.67

Previously, we found that the brush structure in the polymer monolayer of a strongly ionic polyelectrolyte brush was affected by salt added at a critical salt concentration.[17] Even with added salt, if the salt concentration in the water phase is less than the effective ion concentration in the brush layer, then the nanostructure of the brush and even the whole structure of the monolayer are not influenced by the added salt. Beyond the critical salt concentration, the small ions of added salt entered the brush layer, and the brush chains shrunk by the shielding effect on the electrostatic repulsion between ionic brush chains. However, the effect was evaluated only in the carpet + brush system.

In this study, in situ X-ray reflectivity was used to determine the effect of salt on the nanostructure of the carpet-only layer and the critical brush density of the strongly ionic amphiphilic diblock copolymer, poly(hydrogenated isoprene)-*block*-poly(styrenesulfonate sodium salt) (PIp-h$_2$-*b*-PSS). The nanostructure of the carpet-only layer, in which most of the counterions are expected to be condensed, has not been reported. Here we report that, as expected, the monolayer with only a carpet layer did not show any dependence on added salt. We also compared the critical brush density in the present system with the value that we previously found for a weak acid polymer.

Experimental Section

Materials and Polymer Synthesis. The PIp-h$_2$-*b*-PSS diblock copolymers were synthesized as reported previously.[17] Polyisoprene-*b*-polystyrene (PIp-*b*-PS) diblocks have been synthesized by living anionic polymerization. After hydrogenation of the PIp blocks (about 90% 1−4 addition with 9−10% 3−4 addition), sulfonation of the polystyrene (PS) block was performed to obtain the polymers desired. Table 1 shows the characteristics of the polymers thus synthesized. The methods of characterization and purification were as described previously.

***π*−*A* Isotherm Measurement.** For the surface pressure−area per molecule (*π*−*A*) isotherm measurements, we used a Controller FSD-220 and a Langmuir−Blodgett (LB) trough (130 mm × 60 mm) made of aluminum coated with Teflon (USI System, Fukuoka, Japan). The sample copolymer was dissolved in chloroform to prepare a 2.4 mg/mL solution that was then spread on the water surface in the LB trough with a microsyringe to prepare the monolayer. We used Milli-Q ultrapure water and a 0.001 M sodium phosphate aqueous solution as the subphase for pH adjustment, which resulted in counterion exchange of the SO_3^- group from H^+ to Na^+. That is, the hydrophilic segment, PSS, was transformed into sodium polystyrene sulfonate (PSSNa). Thirty minutes was allowed for solvent evaporation, and then the surface was compressed by moving a Teflon barrier at a rate of 0.01 mm/s. The measurements were performed at room temperature.

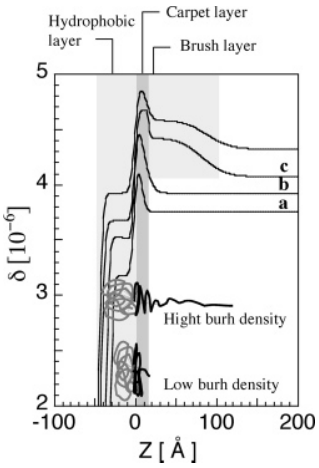

Figure 2. *δ* profiles obtained by box-model fitting for (Ip-h$_2$)$_{220}$-*b*-(SS)$_{55}$ monolayers on water. Each curve was shifted downward to avoid superposition.

X-ray Reflectivity Measurement. The nanostructure of the monolayer on the water surface was directly investigated by in situ X-ray reflectivity (XR) measurements. The XR measurements were performed with an RINT-TTR-MA (Rigaku Corp., Tokyo, Japan) in which the X-ray generator and detector rotate vertically around the sample stage. The specially designed LB trough (130 mm × 60 mm) was mounted on the sample stage. Details of the XR apparatus and data analysis, including fitting quality,[23,26] have been fully described elsewhere.[30−32]

(30) Yamaoka, H.; Matsuoka, H.; Kago, K.; Endo, H.; Eckelt, J. *Physica B* **1998**, *248*, 280.
(31) Kago, K.; Matsuoka, H.; Endo, H.; Eckelt, J.; Yamaoka, H. *Supramol. Sci.* **1998**, *5*, 349.
(32) Matsuoka, H.; Mouri, E.; Matsumoto, K. *Rigaku J.* **2001**, *18*, 54.

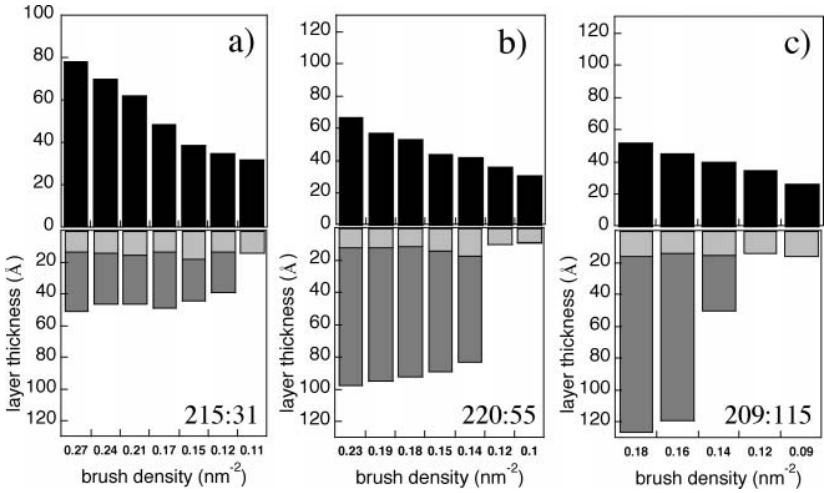

Figure 3. Thickness of the PIp-h_2 layer (filled bar), the PSS carpet layer (gray bar), and the PSS brush layer (open bars) as a function of brush density for (a) $(Ip\text{-}h_2)_{215}$-*b*-$(SS)_{31}$, (b) $(Ip\text{-}h_2)_{220}$-*b*-$(SS)_{55}$, and (c) $(Ip\text{-}h_2)_{209}$-*b*-$(SS)_{115}$ monolayers on water at various surface pressures.

Table 2. Nanostructure of the $(Ip\text{-}h_2)_{220}$-*b*-$(SS)_{55}$ Monolayer on Water at Various Surface Pressures Determined by XR

π (mN/m)	$\delta_{Ip-h2} \times 10^6$	d_{Ip-h2} (Å)	σ_{Ip-h2} (Å)	$\delta_{SSNa1} \times 10^6$	d_{SSNa1} (Å)	σ_{SSNa1} (Å)	$\delta_{SSNa1} \times 10^6$	δ_{SSNa2} (Å)	σ_{SSNa2} (Å)	$\delta_{H_2O} \times 10^6$	σ_{H_2O} (Å)	brush stretch(%)
2		31	3	4.56	9	4	*a*	*a*	*a*		6	5
5		36	4	4.47	10	3	*a*	*a*	*a*		9	6
10		42	4	4.17	17	4	3.92	66	2		23	60
15	3.17	44	4	4.80	14	5	3.83	75	6	3.57	23	67
20		53	3	4.30	11	5	3.92	81	4		23	71
25		57	4	4.29	12	5	3.96	83	10		23	76
30		67	4	4.29	12	6	4.07	85	6		30	78

[a] No brush data because it was fitted by a two-box model. δ for the hydrophobic layer and water subphase were kept constant for all the conditions.

Results and Discussion

Critical Brush Density. We previously found the critical brush density for a weakly ionic polyelectrolyte brush at the air/water interface by using poly(diethylsilacyclobutane)-*b*-poly(methacrylic acid) (PEt_2SB-*b*-PMAA).[27] The PMAA brush density was changed and controlled by blending a carboxylic acid-endcapped poly(Et_2SB) homopolymer into the diblock copolymer and changing the surface pressure. These results suggested that the critical brush density (i.e., the grafting density where the brush layer formed) was independent of the hydrophobic layer thickness. Hence, in this study, we adjusted the brush density of PIp-h_2-*b*-PSS by changing only the area per molecule *A* (i.e., surface pressure π).

Figure 1a shows the X-ray reflectivity profiles of the investigated system, the $(Ip\text{-}h_2)_{220}$-*b*-$(SSNa)_{55}$ monolayer on the water surface. The X-ray reflectivity measurement was taken along the isotherm given in the inset. The electron density profiles of the monolayer normal to the surface were evaluated from XR profiles as a function of brush density to characterize monolayer structure (Figure 2).

The reflectivity analysis was based on the theory of Parratt[33] and Sinha[34] et al. The adjustable parameters in box-model fitting were the density, thickness of each layer, and roughness of each interface. The fitting parameters for the PIp-h_2 layer were fixed at the best-fit value with two-box model fitting because the PIp-h_2 layer thickness was the most reliable parameter obtained by the two-box model. Then, three-box model fitting was first carried out under the condition that the fitting parameters were limited to the density, thickness, and roughness of the two PSS layers. The PSS density parameter was limited up to the bulk PSS density at this stage. Subsequently, the parameters for PIp-h_2 were also fitted. Note that model fitting was carried out in a smaller *q* range ($q < 0.33$ Å^{-1}) with good statistics and the fitting quality in this range was estimated to be ca. 2% with respect to the *R* value[23].

Curve a (0.10 nm^{-2}) in Figure 1a could be reproduced by the two-box model, which means that the monolayer consists of only a hydrophobic layer on water and a 10−20-Å-thick layer of high electron density flatly absorbed to the hydrophobic layer. However, curves b (0.12 nm^{-2}) and c (0.15 nm^{-2}) could not be well reproduced by a two-box model, especially in the low-*q* region, but satisfactory agreement was obtained by using a three-box model. Figure 1b is a magnification of the small-angle regions for these three curves. It is obvious that at graft density >0.12 the three-box model gives us satisfactory agreement whereas the two-box model does not. This means that the monolayer under these conditions consists of three layers. The structural parameters thus estimated are listed in Table 2. The thickness of each layer was plotted as a histogram in Figure 3b as a function of brush density, which was calculated from PIp-h_2 layer thickness, together with corresponding XR profiles and fitting curves for the three polymers used. The hydrophobic PIp-h_2 block showed a linear increase in thickness when compressed. However, the hydrophilic PSS layer showed an interesting dependence on brush density. For the PSS layer over a large molecular area (in other words, at a low brush density), we observed a layer 10−20 Å thick with a high electron density that we call the carpet layer beneath the hydrophobic layer. On further compression, at $\pi =$ 10 mN/m for example, we found two polyelectrolyte layers. Besides the carpet layer, there was a brush layer, a swollen PSS chain layer below the carpet. This is certainly the transition from the carpet-only structure to the carpet + brush double-layer structure as a result of the change in the brush density. The brush

(33) Parratt, L. G. *Phys. Rev.* **1954**, *95*, 359.
(34) Sinha, S. K.; Sirota, E. B.; Garoff, S.; Stanley, H. B. *Phys Rev. B* **1988**, *38*, 2297.

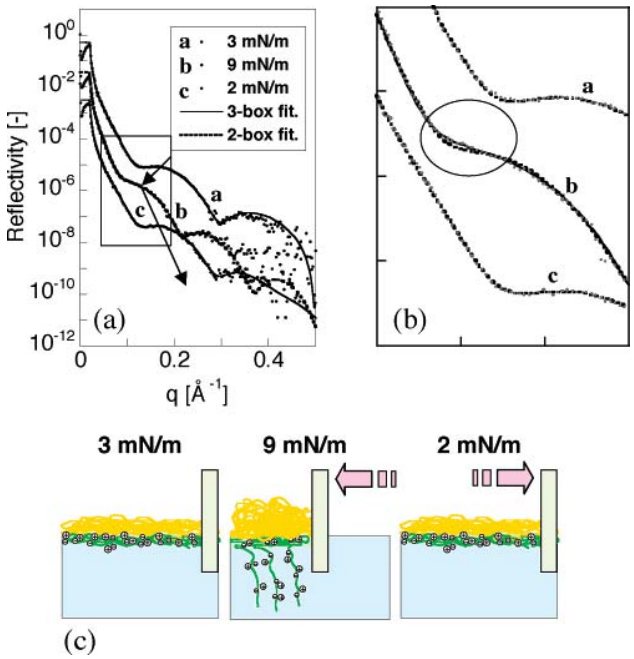

Figure 4. (a) XR profiles for $(Ip\text{-}h_2)_{215}$-*b*-$(SS)_{31}$ monolayers on water at three different surface pressures. The profiles were shifted downward by one decade, and this shows the reversibility of brush layer formation. (b) Magnification of part a in a small-*q* range showing the difference between two fitting models. (c) Schematic representation of the nanostructure change with changing brush density.

chains are stretched to up to 70% of their contour length. From these density profiles, the critical brush density, where a swollen brush layer is formed, for $(Ip\text{-}h_2)_{220}$-*b*-$(SSNa)_{55}$ can be estimated to be about 0.12 nm^{-2}. Thus, the existence of a critical brush density for a strong polyelectrolyte brush at the air/water interface has been confirmed, and its absolute value could be successfully determined.

Reversibility of PSS Brush Layer Formation. To check the reversibility, we prepared a monolayer of $(Ip\text{-}h_2)_{215}$-*b*-$(SSNa)_{31}$ at 3 mN/m and carried out the XR measurement (Figure 4). Curve a in Figure 4 could be reproduced by the two-box model, which means that there is only a carpet layer beneath the hydrophobic layer but no brush layer formation. When the monolayer was compressed to 9 mN/m, we confirmed the brush layer formation in addition to the carpet layer. Notice that curve b in Figure 4b (magnification of the small-angle regions in Figure 4a) could better reproduced by the three-box model than the two-box model. Then, we decompressed the monolayer until the surface pressure reached 2 mN/m. By XR profiles in Figure 4, only carpet-layer formation was confirmed by the structural parameters listed in Table 3. As shown by the schematic representation in Figure 4c, this is a transition from the carpet + brush double-layered structure to the carpet-only structure by decompression. The structural transition between only the carpet-layer structure and the carpet + brush structure was confirmed to be a reversible process at least under 25 °C at a compression rate of 0.01 mm/s.

PSS Chain Length Dependence of the Critical Brush Density. Similar experiments were performed for polymers with different PSS chain lengths but with almost the same hydrophobic PIp-h_2 chain length (m/n = 215:31, 220:55, 209:115; Table 1). We found that they have a similar critical brush densities at around 0.12 nm^{-2} (Fig. 3). This means that the formation of a brush layer in PIp-h_2-*b*-PSSNa depends on the distance between polymer chains (0.34 nm at 0.12 nm^{-2}) but not on the capacity of the carpet, which was thought to be the origin of the transition of the weak acid polymer.[27]

Comparison between Weak and Strong Ionic Groups. Previously, we estimated the critical brush density of weakly ionic amphiphilic diblock copolymer, $(Et_2SB)_m$-*b*-$(PMAA)_n$, to be 0.48 chains/nm^2 for m/n = 34:50 [27(a)]. In this study, the critical brush density for a strong polyelectrolyte brush of PIp-h_2-*b*-PSSNa with the same hydrophilic unit showed a transition at 0.12 nm^{-2}, which is smaller than that for $(Et_2SB)_{34}$-*b*-$(PMAA)_{50}$. This may mean that the brush was formed more easily with the strong acid chain than with the weak acid chain. Brush formation might be accelerated by the electrostatic repulsion between neighboring segments on the PSS chain, which will stretch the chain. The reason for the difference in the hydrophilic chain length dependence of the critical brush density remains unknown. We previously attributed the dependence to the capacity of the carpet layer whose thickness is independent of both the hydrophilic chain length and brush density in a weak polyelectrolyte brush. The present observation in a strong polyelectrolyte (i.e., no dependence on PSS chain length) suggests that the electrostatic interaction between brush chains is the dominant factor for brush formation because of its strongly ionic nature.

Relationship between the Collapse Point and the Debye Length. When the monolayer was further compressed to make a higher brush density, it eventually collapsed. We expected that if the destruction of the brush structure caused the collapse then the interbrush chain distance at the collapse point would be related to the Debye length for the PSS chain in the brush layer. The

Table 3. Nanostructure of the $(Ip\text{-}h_2)_{215}$-*b*-$(SS)_{31}$ Monolayer on Water at 9 and 2 mN/m Determined by XR

surface presssure (mN/m)	δ_{Ip-h2} × 10^6	d_{Ip-h2} (Å)	σ_{Ip-h2} (Å)	δ_{SSNa1} × 10^6	d_{SSNa1} (Å)	σ_{SSNa1} (Å)	δ_{SSNa1} × 10^6	δ_{SSNa2} (Å)	σ_{SSNa2} (Å)	δ_{H_2O} × 10^6	σ_{H_2O} (Å)
9	3.17	43	5	3.92	18	3	3.67	25	5	3.57	9
2	3.17	31	4	4.13	14	4	*a*	*a*	*a*	3.57	4

[a] No brush data because it was fitted by a two-box model.

Table 4. Effect of Added Salt to the $(Ip\text{-}h_2)_{220}$-*b*-$(SS)_{55}$ Monolayer on Water at 5 mN/m Determined by XR

C_S (mol/L)	δ_{Ip-h2} × 10^6	d_{Ip-h2} (Å)	σ_{Ip-h2} (Å)	δ_{SSNa1} × 10^6	d_{SSNa1} (Å)	σ_{SSNa1} (Å)	δ_{SSNa1} × 10^6	δ_{SSNa2} (Å)	σ_{SSNa2} (Å)	δ_{H_2O} × 10^6	σ_{H_2O} (Å)
0		36	4	4.47	10	3	*a*	*a*	*a*	3.57	9
0.1		36	4	4.10	11	3	*a*	*a*	*a*	3.57	8
0.2	3.17	34	4	4.29	9	4	*a*	*a*	*a*	3.59	8
0.3		38	3	4.11	12	3	*a*	*a*	*a*	3.60	5
1		35	3	4.27	14	3	*a*	*a*	*a*	3.65	6
2		36	3	4.44	13	3	*a*	*a*	*a*	3.74	10

[a] No brush data because it was fitted by a two-box model. δ for the hydrophobic layer was kept constant for all the conditions.

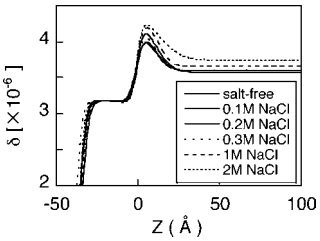

Figure 5. δ profiles obtained by three-box model fitting for (Ip-h_2)$_{220}$-*b*-(SS)$_{55}$ monolayers on water containing NaCl at various concentrations in the subphase at 5 mN/m.

Debye length in the brush layer was 0.68 nm for 55 units of PSS, using the effective free ion concentration in the brush layer of 0.2 M, which was determined by the critical salt concentration study.[17] From the $\pi-A$ data, the distance between polymer brush chains was calculated to be about 0.7 nm, which is close to the Debye length calculated above. This supports the view that the enhanced strong electrostatic repulsion between brush chains is the origin of the collapse of the monolayer by compression.

Effect of Salt on the Carpet-Layer Comparison between Monolayers with and without Brush Layers. As reported previously,[17] salt has an effect only when the added salt concentration is higher than the intrinsic effective concentration of counterions in the brush layer. We call this salt concentration, where transition occurs, the critical salt concentration. From this value, we evaluated the degree of ion condensation in the brush layer. In this study, we carried out the same experiment for the monolayer with a carpet-only layer (i.e., no brush layer) to calculate the degree of ion condensation in the carpet.

The X-ray reflectivity measurements were taken at a surface pressure of 5 mN/m. The electron density profiles of the (Ip-h_2)$_{220}$-*b*-(SSNa)$_{55}$ monolayer with various salt concentrations in the subphase solution were evaluated from XR profiles as a function of salt concentrations (Figure 5). The fitting parameters are shown in Table 4. As the result, no change was observed at 5 mN/m in the density profiles even at a salt concentration as high as 2 M.

When salt ions enter the brush, the electrostatic interaction between PSS chains is screened and results in both a decrease in surface pressure and shrinking of the brush chains.[17] However, in the case of the carpet-only layer, neither a change in surface pressure nor a change in layer thickness was observed. Note that in a previous work on the effect of salt addition to the monolayer with carpet + brush layers we obtained a similar result for the carpet layer. The brush shrunk when the subphase salt concentration increased because of the screening effect, but the thickness of the carpet layer was not influenced by the addition of salt and was kept constant at about 15−20 Å. This indicated that most of the counterions in the carpet layer are strongly condensed and no free counterion exists in the carpet layer. In this study, we confirmed that such a characteristic is independent of the existence of the brush layer. Naturally, we believe that counterion condensation is the origin of the insensitivity of the carpet layer to salt addition. Otherwise, the carpet structure itself would be destabilized and destroyed by the electrostatic repulsion between ionic chains in the carpet layer. The present study is the first experimental evidence of this situation.

This result is also a compelling argument for the existence of the critical brush density according to the very different sensitivity against salt addition between carpet-only and carpet + brush monolayers. The salt unaffectedness of the carpet-only monolayer confirmed the absence of the brush layer, and this critical transition is related to the costs of data treatment procedures.

Conclusions

The critical brush density, effect of salt on the carpet layer, and reversibility of the carpet-only/carpet + brush double-layer structure were investigated by an in situ X-ray reflectivity technique for the PIp-h_2-*b*-PSS monolayer on the water surface. The critical brush density, where the brush layer was formed in addition to the carpet layer, was estimated to be 0.12 chains/nm^2, independent of PSS chain length. This value was smaller than that obtained in a weak ionic amphiphilic diblock copolymer, (Et_2SB)$_{34}$-*b*-(PMAA)$_{50}$ (0.48 chains/nm^2). The distance between PSS brush chains at the critical brush density was found to be 0.34 nm. This value is almost equal to half of the Debye length calculated from the concentration of free counterions in the brush layer and suggests the presence of electrostatic interactions in brush formation. The reversibility of the carpet-only/carpet + brush structure transition is also confirmed.

This study revealed that the structure of the carpet layer is independent of salt concentration in the carpet-only structure as in the double-layer structure. This finding suggests that the degree of condensation counterions in the carpet layer is very high even for a strong polyacid. Therefore, information on the nanostructure of a strong polyelectrolyte brush obtained in this study is highly valuable for a correct understanding of polyelectrolyte brush formation together with those for weak polyelectrolyte brushes.

Acknowledgment. This work was supported by a grant-in-aid for scientific research (nos. A14045244 and A15205017) from the Ministry of Education, Culture, Sports, Science and Technology of Japan, to whom our sincere gratitude is due. This work was also supported by the Sasakawa Scientific Research Grant from The Japan Science Society and the 21st Century COE Program, COE for a United Approach to New Materials Science.

LA061444X